PCCP

First-Principles Predictions for Shear Viscosity of Air Components at High Temperature

Journal:	*Physical Chemistry Chemical Physics*
Manuscript ID	CP-ART-01-2023-000072.R1
Article Type:	Paper
Date Submitted by the Author:	27-Feb-2023
Complete List of Authors:	Valentini, Paolo; University of Dayton Research Institute, Verhoff, Ashley; Air Force Research Laboratory Grover, Maninder; University of Dayton Research Institute Bisek, Nicholas; Air Force Research Laboratory

PCCP

ARTICLE TYPE

Cite this: DOI: 00.0000/xxxxxxxxxx

First-Principles Predictions for Shear Viscosity of Air Components at High Temperature†

Paolo Valentini,*[a] Ashley M. Verhoff,[b] Maninder S. Grover, [a] and N. J. Bisek [b]

Received Date
Accepted Date

DOI: 00.0000/xxxxxxxxxx

The direct molecular simulation (DMS) method is used to obtain shear viscosity data for non-reacting air and its components by simulating isothermal, plane Poiseuille subsonic flows. Shear viscosity is estimated at several temperatures, from 273 K to 10000 K, by fitting the DMS velocity profiles using the analytic solution of the Navier-Stokes equations for this simple canonical flow. The *ab initio* potential energy surfaces (PESs) that describe the various atomic-level interactions are the only input in the simulations. Molecules involved in a collision within the flow can occupy any rovibrational state that is allowed by the effective diatomic potential. For molecular nitrogen, oxygen, and air at standard condition molar composition, the DMS shear viscosity predictions are in excellent agreement with the experimental data that are available up to about 2000 K. The results for pure molecular nitrogen and pure molecular oxygen also agree very well with previously published quasi-classical trajectory (QCT) calculations based on the same PESs. It is further shown that the *ab initio* shear viscosity data are generally lower than the corresponding values used in popular computational fluid dynamics codes, over a wide temperature range. Finally, Wilke's mixing rule is demonstrated to accurately predict the DMS air viscosity results from the pure molecular components data up to 4000 K.

1 Introduction

The need for accurate transport models for air at high temperature is particularly important for hypersonic flight. Typical shock layer temperatures often exceed thousands of degrees in the vicinity of the stagnation point of a hypersonic vehicle and can also be quite high near the entire surface for sustained hypersonic cruising[1]. The experimental characterization of transport properties for air and its constituents beyond about 1000 K becomes extremely difficult and is affected by considerable uncertainty[2–7]. Therefore, molecular simulation offers an attractive theoretical alternative to experiments, particularly when employed with *ab initio* potential energy surfaces (PESs) that describe atomic-level interactions between the various air particles[8–16].

Most studies based upon these first-principles PESs have focused on kinetic processes involving internal energy relaxation and its coupling to chemical reactivity[9,17–20], with considerable success in validating the results with the available experimental data. However, less work has been done to investigate their ability to predict transport properties. Only recently, studies have been conducted to obtain transport phenomena from first-principles potential surfaces. Although shear viscosity has received some particular attention[21–24], we devised a novel approach using the direct molecular simulation (DMS) method to estimate thermal conductivity from *ab initio* PESs[25].

State-of-the-art collision integrals used in computational fluid dynamics (CFD)[26,27] were also derived from molecular interaction models. However, with the exception of monoatomic systems, these simplified potentials[28,29] have disparate accuracy (from semi-empirical to phenomenological) and origin (being obtained from quantum mechanical methods of various accuracy). Although not necessarily inaccurate, many physical interactions between diatoms were often modeled too simplistically[28] (i.e., point-mass assumptions neglecting internal degrees of freedom). Furthermore, many simplified potentials were calibrated using low-temperature shear and bulk viscosity data, thus making their transferability to high temperatures questionable. Our approach is to derive physical and chemical properties for air from a *consistent* set of *ab initio* surfaces obtained from methods of similar accuracy. Importantly, *no empirical information from shear viscosity measurements is built into these PESs, as the interatomic energies are exclusively computed from first-principles methods.*

This study represents a refinement and extension of our previous efforts[24,30] that were targeted to obtain shear viscosity data for atomic and molecular nitrogen from *ab initio* potential energy surfaces. Similar to our previous works, we use the DMS method to simulate canonical, two-dimensional, laminar gas flows from which the shear viscosity coefficient is obtained. Here, we ex-

[a] *University of Dayton Research Institute, 1700 South Patterson Blvd, Dayton, Ohio 45469, USA; E-mail: pvalentini1@udayton.edu.*
[b] *US Air Force Research Laboratory, Wright-Patterson Air Force Base, Dayton, Ohio 45433, USA.*

tend the previous results to molecular and atomic oxygen as well as mixtures of molecular nitrogen and oxygen at standard condition composition, for a wide range of temperatures. In addition, we present a rigorous procedure to quantify the statistical uncertainty on the molecular simulation data.

The DMS method is closely related to the direct simulation Monte Carlo (DSMC) method[31]. However, the simplified collision models used in DSMC are all replaced by molecular dynamics trajectories on a PES. In other words, DMS combines the efficiency of the DSMC technique with the accuracy of trajectory-based calculations, such as the quasi-classical trajectory (QCT) method[32]. The QCT method has been routinely used to evaluate transport properties, but it must be based on a Monte Carlo quadrature of the relevant collision integrals[33]. For diatom-diatom systems, because of the high dimensionality of the reactants' configuration space, several simplifying assumption must be used to make the calculations computationally tractable. For example, Mankodi *et al.*[21] present QCT-obtained data for shear viscosity of molecular nitrogen and oxygen, but they consider reactant molecules in the ground rotational state only and having different vibrational states. Previously, we found very good agreement between DMS predictions for molecular nitrogen shear viscosity[30] and the data presented by Mankodi *et al.*[21], where both sets of results were based upon the same potential energy surface of Paukku *et al.*[8,9]. However, this conclusion cannot be extended in general.

In our approach, the DMS method is used to compute a plane, isothermal Poiseuille flow. Although the DMS method allows for all collision outcomes consistent with the local gas state, as discussed later, the specified chemical composition is not allowed to change in this work. The total collision energy is redistributed between translational and internal energy depending on the phase-space region explored during the interaction. For systems characterized by multiple PESs due to their unpaired electrons (e.g., ground-state O_2+O_2), interactions occur on the relevant set of PESs with the appropriate statistical weights related to the overall spin couplings. We point out that the results presented by Mankodi *et al.*[21] for molecular oxygen were obtained from trajectories on the triplet ground-state O_2+O_2 surface only. Finally, we estimate the shear viscosity of the gas by using the known analytic solution for the flow. The procedure is repeated at various gas flow temperatures, thus yielding shear viscosity as a function of temperature.

The objective of this work is two-fold. First, we report shear viscosity data obtained from DMS based on *ab initio* PESs removing some of the simplifying assumptions utilized in previous works based on some of the PESs employed in this work. The results presented here are also rigorously assigned proper confidence intervals. Second, the method described in this work is independent of the particular intermolecular models and gas compositions. Therefore, arbitrary multi-component gas flows could be simulated with DMS to obtain shear viscosity data for an arbitrary gas mixture, whereas a mixing rule would be needed in QCT calculations, i.e., another modeling assumption.

This article is organized as follows: in Sec. 2, we briefly describe the main numerical ingredients (Sec. 2.1), the intermolecular models (Sec. 2.2), and the simulation parameters (Sec. 2.3). The uncertainty quantification is discussed in Sec. 2.4. Results are discussed in Sec. 3, where nitrogen (Sec. 3.1), oxygen (Sec. 3.2), and air (Sec. 3.3) shear viscosity data from DMS are presented. Finally, the conclusions are stated in Sec. 4.

2 Methodology

2.1 Direct molecular simulation

Only a brief overview of the DMS method is provided here, as it has been extensively described in previous references[17–20,34–36]. As stated, the DMS method and DSMC share the same formulation, with the exception of the mapping from initial (reactant) to final (product) molecular states. In DSMC, this mapping is obtained from functions of a set of pre-collision quantities (e.g., total collision energy, impact parameter, initial states, etc.). Instead, the DMS method directly utilizes a trajectory integration to obtain the post-collision states (i.e., product states).

Similar to DSMC, DMS simulations are carried out using time steps of the order of the smallest mean collision time in the flow, the cell sizes in the flow field are of the order of the local mean free path, and only a subset of real particles in each control volume is simulated by assigning a so-called particle weight. The no time counter (NTC) algorithm[31] is used to select particle pairs for collisions in each cell[34]. A sufficiently large hard-sphere total cross-section $\sigma = \pi b_{max}^2$ based upon the maximum impact parameter b_{max} is used to conservatively ensure that all collisions having a non-negligible angle of deflection are simulated. This is particularly important for transport coefficients since they are functions of integrals of the scattering angle over all impact parameters[33].

DMS particles possess all the internal phase-space coordinates needed to describe their structure (e.g., single atoms, diatomics, triatomics, etc.). When selected for trajectory integration, their coordinates are propagated in time by integrating Newton's second law of motion using the finite-difference, symplectic velocity-Verlet algorithm[37], with a time step of the order of a femtosecond. Trajectories are truncated when the products are separated by a distance D_0 which is large enough that no effective state changes are possible. All simulation parameters are detailed in Sec. 2.3.

2.2 Ab initio potential energy surfaces

Molecular interactions are modeled with *ab initio* PESs. All PESs are listed in Table 1 for each interaction together with the references containing the computational details of the quantum mechanical methods[8–11,14]. In general, the authors[8–11,14] used complete active space second-order perturbation theory (CASPT2) using a minimally augmented correlation-consistent polarized valence triple zeta basis set (maug-cc-pVTZ). A complete active space self-consistent-field (CASSCF) calculation was generally used to obtain orbitals and a reference state for the CASPT2 calculations. Many thousands of single-point energies were then fit using permutationally invariant polynomials to obtain smooth surfaces suitable for dynamical calculations, such as those presented in this work. For N_2+N_2 and N_2+O_2 collisions, trajectories are integrated on the respective PESs. However, for molecular oxygen collisions, trajectories occur on one of three surfaces (Table 1), with probability 1/9 (singlet), 3/9 (triplet) and 5/9 (quintet).

Dissociation energy curves are used for atom-atom trajectories.

No electronic excitation is considered in this work because trajectories occur on ground-state PESs only. A precise estimate of the error resulting from neglecting electronically excited states, which are known to be important at high temperature[38], is made difficult by the current lack of PESs for electronically excited states. The method presented here is not inherently limited to adiabatic dynamics only, thus it can be extended to non-adiabatic dynamics as new, accurate electronic structure calculations are conducted[39]. Furthermore, collision-specific ground-state cross-sections are still needed in kinetic particle methods (e.g., DSMC) for the simulation of hypersonic flows in thermochemical nonequilibrium.

Table 1 *Ab initio* potential energy surfaces

Interaction	Reference(s)
N_2+N_2, N+N	Bender *et al.* [8,9]
O_2+O_2, O+O	Paukku *et al.* (singlet and quintet) [10]
	Paukku *et al.* (triplet) [11]
N_2+O_2	Varga *et al.* [14]

2.3 Simulation details

Isothermal, plane Poiseuille flows were simulated with DMS to estimate the shear viscosity coefficient using the Navier-Stokes analytic solution for the steady-state velocity profile $v(x)$:

$$v(x) = -\frac{1}{\eta}\frac{x(L-x)}{2}\frac{dp}{dy}, \quad (1)$$

where η is the shear viscosity, and L is the separation between two infinite flat plates in the yz plane[40]. The pressure gradient along y, $\frac{dp}{dy}$, drives the flow and was obtained by imposing a constant acceleration, a_y, in the y direction. This body force results in a pressure gradient $-\frac{dp}{dy} = a_y\rho$, with ρ the mass density of the gas. The magnitude of a_y was adjusted to minimize compressibility effects, so that the Mach number based on the maximum speed in the channel, $v(L/2)$, would not exceed about 0.3 at the imposed wall temperature. This resulted in nearly isothermal flows. The channel width L was set to 1×10^{-5} m. Periodicity was enforced in the y and z directions. For all cases, the number density was set to 4.2×10^{25} m^{-3}, corresponding to a mass density between 1 and 2.2 kg/m^3, depending on the gas composition. The corresponding Reynolds numbers varied from about 20 to 150, depending on temperature and gas, and, thus, the stable, time-invariant solution contained in Eq. 1 is expected to describe the channel flow velocity profiles.

For trajectory integration, the time step was varied from 0.05 fs to 1 fs, with smaller values at the higher temperatures. Each trajectory was integrated using the velocity Verlet algorithm with a fixed time step. The maximum impact parameter b_{max} was set to 6 Å for all cases, whereas D_0 was set to 15 Å for N and N_2, 20 Å for O and 25 Å for O_2. We found that oxygen interactions extended to larger separations than in nitrogen, thus requiring a bigger spatial cut-off D_0.

Particle-wall interactions were modeled as fully diffuse. Molecules impinging on the walls were reflected with no dependence on their incident velocity and were given a new center-of-mass velocity vector, sampled from a Gaussian distribution consistent with the surface temperature. Both walls were maintained at the same temperature. For molecules, their internal phase-space coordinates were assigned to correspond to internal energies (rotational and vibrational) distributed according to a Boltzmann distribution consistent with the wall temperature and diatomic energy curve, and without any correlation with the internal states prior to the collision with the wall. To ensure consistency with the classical dynamics of interactions between molecules in the interior of the simulation domain, vibrational states of the wall-scattered molecules were assigned using fractional vibrational states for each of the allowed rotational states, using the Wentzel-Kramers–Brillouin (WKB or quasi-classical) approximation[32]. Specifically, each vibrational level at a given rotational state was subdivided into 20 sub-levels, thus better approximating a continuous distribution of vibrational states, starting from the minimum of the potential well (i.e., no zero-point energy was included in the generation of states for wall-reflected molecules). Finally, we point out that the gas behavior in the vicinity of the walls did not correspond to any realistic atomic-level interaction. A *realistic* treatment of particle-wall collisions would introduce numerous difficulties. First, the assumption of atomically flat surfaces becomes questionable (and, in most cases, incorrect) for most materials at high temperatures. Second, PESs describing molecule-wall interactions are, in most cases, unavailable for arbitrary surface materials exposed to air or its components. Third, adsorption/desorption of gas molecules on the channel walls as well as surface coverage would have to be incorporated in the simulations to achieve better realism. Clearly, these are only some of the important aspects of gas-surface interactions in high-temperature gas flows, but they are beyond the scope of the present study. Here, the walls simply imposed complete thermal and velocity accommodation, resulting in a near no-slip wall boundary condition that enables a comparison with the analogous continuous flow described by the Navier-Stokes equations. Therefore, the data presented here should be interpreted as consistent with the Chapman-Enskog hydrodynamics.

Finally, to maintain the initial chemical composition of the molecular systems, we ignored all simple and double dissociations by resetting the phase-space coordinates of the colliding molecules to their initial pre-collision states if they underwent dissociation. Note that exchange reactions were permitted in the case of N_2+N_2 or O_2+O_2 collisions, as they do not alter the chemical composition of the system. For N_2+O_2 interactions, exchange processes would result in NO production, and, thus, they were forbidden. Hence, the gas was generally in local thermal equilibrium, but not in chemical equilibrium. Similarly, for atomic systems, the DMS method ignores recombination since only pairwise interactions are allowed. Therefore, the system remained in thermal equilibrium only.

2.4 Uncertainty estimation

Similar to other particle methods, DMS predictions of macroscopic observables are affected by several sources of uncertainty. These can be grouped into three main categories: (i) PES accuracy, (ii) simulation parameters (e.g., trajectory integration time step, NTC time step, cut-offs, etc.), and (iii) statistical uncertainty.

It is beyond the scope of this work to analyze the uncertainty deriving from the PES. Previous works have attempted to establish comparisons between predictions from independently derived PESs on the same macroscopic observables and, therefore, draw conclusions on their accuracy[30,41,42]. Uncertainty quantification was also conducted for select potential surfaces[43]. Unfortunately, these investigations are often made difficult by the lack of experimental data with sufficient resolution to discern between *ab initio* predictions or the altogether lack of experimental data, particularly at very high temperatures.

Simulation parameters may introduce systematic errors in the molecular simulation results. A judicious choice of these parameters was made to minimize their impact on the uncertainty affecting the reported data. In select cases, simulations were repeated with more conservative values and the invariance of the results (within statistical scatter) was verified.

The use of Eq. 1 to estimate the shear viscosity η from the velocity profile is strictly valid at steady-state. Figure 1(a) shows the transient from the (arbitrary) initial condition to the steady state flow. We observed that the relaxation time to steady state was of the order of microseconds for the temperature and density conditions chosen in this work. Hence, cumulative sampling of the velocity profile before the system reaches steady state introduces a systematic error in the time average of $v(x)$ and, consequently, η. On the other hand, very long simulation times that would average out the bias from the initial transient, become excessively expensive, due to the cost of simulating an enormous number of trajectories on *ab initio* PESs. However, as shown in Figure 1(a), the DMS flow transient is time accurate and in close agreement with the numerical solution of the Navier-Stokes equations using the DMS prediction for shear viscosity (obtained at steady state). This is expected provided that the DMS simulation parameters, namely cell size and time step, are chosen appropriately, as briefly described in Sec. 2.1. Therefore, to monitor the evolution of the system to steady state, we extracted velocity profiles at fixed intervals throughout the DMS transient. These samples were collected over intervals of 1000 or 2000 DMS time steps and averaged from all time steps or from every other time step during those intervals. Because the typical DMS time step was set to ~ 1 ps, the velocity samples were averaged over about ~ 1 ns, a small time window in comparison to the characteristic flow time of $\sim 1\mu$s. Therefore, each velocity profile can be considered instantaneous and was fit using Eq. 1 to obtain η from a least-square procedure. In this manner, the time evolution of η was obtained, as shown in the example in Fig. 1(b) for molecular nitrogen at 273 K. The uncertainty on the measurements for η was then assigned as one standard deviation of the samples collected within the steady-state temporal window.

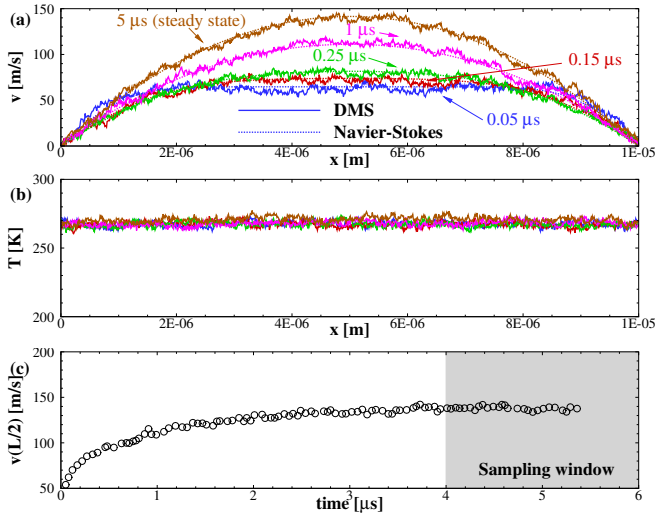

Fig. 1 (a) Time evolution of a 273 K molecular nitrogen plane, Poiseuille flow predicted by the DMS from the initial condition to steady state. The transient is compared to the Navier-Stokes continuum prediction based upon the shear viscosity estimate at steady state using Eq. 1; (b) translational temperature profiles during the transient across the channel; (c) corresponding time evolution of the shear viscosity estimate.

3 Results and discussion

DMS shear viscosity predictions are presented for atomic and molecular nitrogen (Sec. 3.1), atomic and molecular oxygen (Sec. 3.2), and non-reactive air (Sec. 3.3). In all cases, the reported DMS data have an uncertainty of less than 5% assuming a confidence interval of 68%. All data are compared to the zero-density limit experimental correlation of Lemmon and Jacobsen[4]. This correlation was obtained by an extensive analysis of existing experimental data and was generally within 5-6% of the actual experimental data points. For this reason, we use it as a surrogate of the experimental measurements for ease of presentation. It is important to emphasize that experiments are limited to temperatures below about 2000 K, and thus a comparison with the high-temperature extrapolation of the Lemmon and Jacobsen correlation is only meant to highlight the limitations and potential risks of empirical fits. Fits for the DMS data were obtained assuming a power-law dependence of shear viscosity on temperature:

$$\eta(T) = \eta_{\mathrm{REF}} \left(\frac{T}{T_{\mathrm{REF}}} \right)^{\omega}, \qquad (2)$$

where we selected $T_{\mathrm{REF}} = 273.16$ K and where ω is the viscosity index.

DMS shear viscosity predictions for nitrogen and oxygen are also compared with the QCT data of Mankodi *et al.*[21]. For N+N and N_2+N_2 interactions, both sets of results are obtained from precisely the same PES. However, for O_2+O_2, the QCT results were obtained on the triplet surface only[11], which constitutes one of the three possible spin couplings. In our DMS, however, all three surfaces are utilized, as described in Sec. 2.2.

Finally, comparisons are presented between the DMS results for oxygen and nitrogen and the *collision-specific* DSMC cross-section calibrations of Swaminathan-Gopalan and Stephani[26]. In their

work, the authors recommend DSMC parameters that best reproduce the collision integrals currently employed in the Langley Aerothermodynamic Upwind Relaxation Algorithm (LAURA)[44] and Data Parallel Line Relaxation (DPLR)[45] CFD solvers. To compare to their variable hard sphere (VHS) data[26], we used the standard relation:

$$\eta_{\mathrm{REF}} = \frac{15\sqrt{2\pi m_r k_B T_{\mathrm{REF}}}}{2(5-2\omega)(7-2\omega)\pi d_{\mathrm{REF}}^2}, \quad (3)$$

where m_r is the reduced mass and k_B is Boltzmann's constant[31].

3.1 Shear viscosity of atomic and molecular nitrogen

The DMS results for molecular and atomic nitrogen shear viscosity are shown in Fig. 2(a) over the typical experimental temperature range and are extended to 10000 K in Fig. 2(b). For temperatures below approximately 2000 K, the DMS predictions for molecular nitrogen shear viscosity are in excellent agreement with the experimental correlation of Lemmon and Jacobsen[4]. It can be seen that the extrapolation of the experimental correlation is in fair agreement with the calculations up to 4000 K, but significantly over-predicts the molecular shear viscosity at even higher temperatures. Figure 2 also contains the DMS results for atomic nitrogen shear viscosity, for which no available experimental data were found.

Using Eq. 2, a least-square procedure yielded shear viscosity indices ω of 0.688 and 0.663 for N+N and N_2+N_2, respectively. This is in contrast with the commonly used value of 0.74 for molecular nitrogen recommended by Bird[31], that was, however, obtained from shear viscosity data at near standard conditions. The reference viscosity (η_{REF}) was 20.5 μPa s and 17.0 μPa s for N+N and N_2+N_2, respectively. For molecular nitrogen, η_{REF} is within 3% of the value reported by Bird[31].

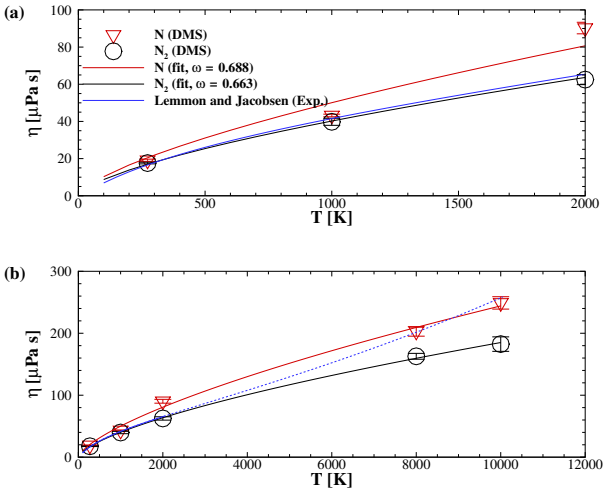

Fig. 2 (a) DMS and experimental shear viscosity data for atomic and molecular nitrogen up to 2000 K; (b) DMS shear viscosity data for atomic and molecular nitrogen up to 10000 K. The dashed line denotes the high-temperature extrapolation of the zero-density limit experimental correlation of Lemmon and Jacobsen[4] for molecular nitrogen.

The comparison between DMS and QCT shear viscosity data is shown in Fig. 3(a) for atomic nitrogen and Fig. 3(b) for molecular nitrogen. For N_2+N_2 interactions, the agreement between the two methodologies is remarkably good over the entire temperature range considered in this study. However, for N+N interactions, the DMS predictions become significantly larger at temperatures greater than about 2000 K, despite being based on the same interatomic potential. The origin of this discrepancy is currently not known.

Shear viscosity data obtained by Istomin and Kustova[38] using the Chapman-Enskog theory and accounting for electronic excitation are presented in Fig. 3(a)-(b) for both atomic and molecular nitrogen. In the temperature range that we considered (273 K to 10000 K), the agreement with the DMS predictions is good, particularly for atomic nitrogen. At temperatures below about 2000 K, the shear viscosity coefficients for molecular nitrogen obtained by Istomin and Kustova[38] are also in excellent accordance with the DMS data. However, at higher temperatures, the DMS shear viscosity results are lower, with a maximum discrepancy of about 15% at 10000 K. This could be attributed to the increasing importance of electronic excitation at very high temperatures.

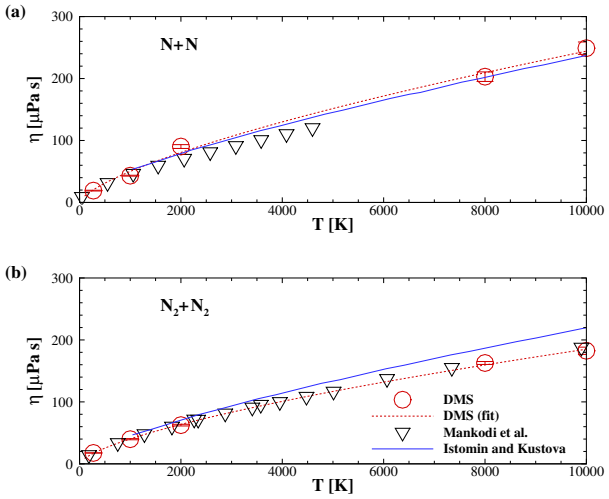

Fig. 3 Comparisons between DMS, QCT[21] and Chapman-Enskog[38] shear viscosity data for nitrogen.

Finally, we show the comparison with the fits of Swaminathan-Gopalan and Stephani[26], who consider both 6-species neutral air (1000 K to 5000 K) and 13-species ionized air (1000 K to 10000 K). As shown in Fig. 4, the DMS data are generally lower than the recommended collision-specific fits, for both atom-atom and diatom-diatom collisions. Better agreement is seen with the neutral air collision parameters, as expected. Table 2 contains the DMS-tuned VHS parameters, namely ω and d_{REF}, with the latter obtained from the expression contained in Eq. 3.

3.2 Shear viscosity of atomic and molecular oxygen

The DMS results for molecular and atomic oxygen shear viscosity are shown in Fig. 5(a)-(b). Similar to molecular nitrogen, the DMS shear viscosity predictions agree remarkably well with the experimental data up to about 1500 K[4]. The extrapolation of the

Table 2 DMS-informed VHS collision-specific reference diameter and viscosity index for nitrogen.

Interaction	d_{ref} (DMS)	d_{ref} (neutral air VHS[26])	ω (DMS)	ω (neutral air VHS[26])
N+N	3.078 Å	2.967 Å	0.688	0.688
N_2+N_2	3.971 Å	3.536 Å	0.663	0.627

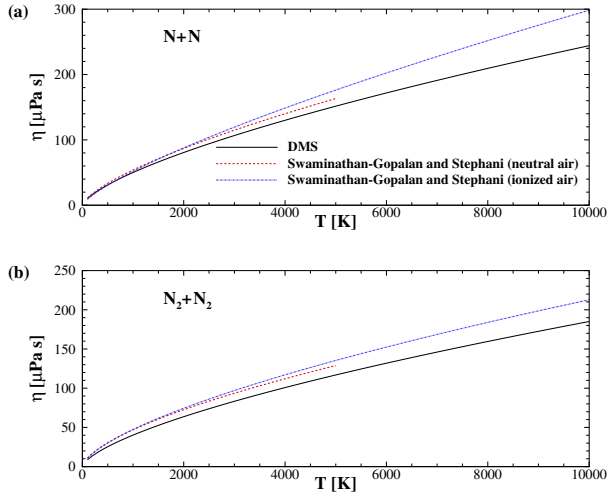

Fig. 4 Comparisons between DMS and VHS[26] nitrogen shear viscosity curve fits.

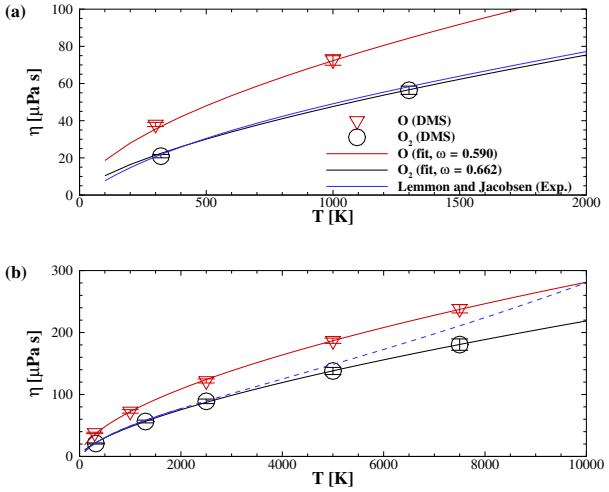

Fig. 5 (a) DMS and experimental shear viscosity data for atomic and molecular oxygen up to 2000 K; (b) DMS shear viscosity data for atomic and molecular oxygen up to 7500 K. The dashed line denotes the high-temperature extrapolation of the zero-density limit experimental correlation of Lemmon and Jacobsen[4] for molecular oxygen.

experimental correlation is shown to predict shear viscosity relatively well up to 5000 K. Beyond that, the high-temperature extrapolation considerably over-predicts the DMS data. For atomic oxygen, the DMS results are qualitatively similar to those obtained for atomic nitrogen, in that the atomic system exhibits larger viscosity than the molecular system. For atomic oxygen, no available experimental data were found. The reference shear viscosity was 33.6 μPa s and 20.2 μPa s for O+O and O_2+O_2, respectively. For molecular oxygen, η_{REF} is within 6% of the value reported by Bird[31].

Similar to atomic nitrogen, the DMS shear viscosity data for O+O interactions are generally larger than the corresponding results from QCT[21], as shown in Fig. 6(a). On the other hand, for molecular oxygen, the agreement is remarkably good over the entire temperature range considered in our work, as illustrated in Fig. 6(b). This is despite several simplifying assumptions used in QCT, that were detailed in the Introduction. More importantly, the QCT data were obtained on the triplet O_2+O_2 surface only. This suggests that all three surfaces (singlet, triplet, and quintet) predict a similar shear viscosity.

Shear viscosity data that include electronic excitation[38] are presented in Fig. 6(a)-(b) for a comparison with the DMS predictions. For atomic oxygen, DMS and Chapman-Enskog theory shear viscosity data are in fair agreement, up to 10000 K, and agree very well for molecular oxygen. Similar to N_2, the shear viscosity obtained by Istomin and Kustova[38] is larger at the higher temperatures, with a maximum discrepancy of about 7% at 7500 K, potentially attributable to electronically excited states.

Like for nitrogen, we report a comparison with the fits of Swaminathan-Gopalan and Stephani[26]. As shown in Fig. 7(a),

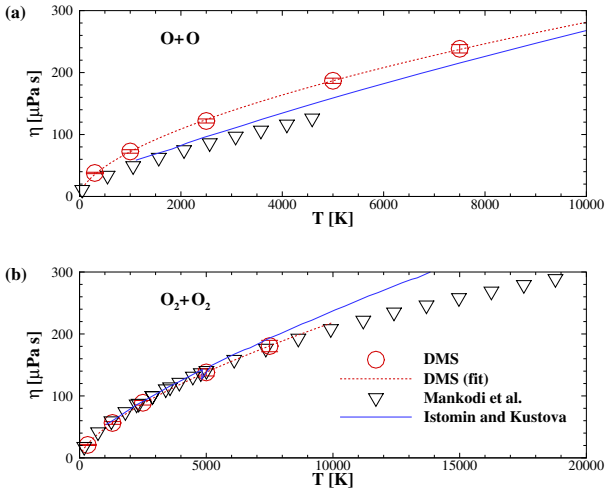

Fig. 6 Comparisons between DMS, QCT[21] and Chapman-Enskog[38] shear viscosity data for oxygen.

the atomic oxygen shear viscosity from DMS is in close agreement with the VHS fits for both neutral and ionized air, but closer to the neutral air curve. Like molecular nitrogen, for molecular oxygen, DMS predicts shear viscosity values that are lower than the corresponding VHS fits from Swaminathan-Gopalan and Stephani[26]. This is illustrated in Fig. 7(b). Table 3 contains the DMS-tuned VHS parameters.

Table 3 DMS-informed VHS collision-specific reference diameter and viscosity index for oxygen.

Interaction	d_{ref} (DMS)	d_{ref} (neutral air VHS[26])	ω (DMS)	ω (neutral air VHS[26])
O+O	2.380 Å	3.005 Å	0.590	0.717
O_2+O_2	3.772 Å	3.380 Å	0.662	0.641

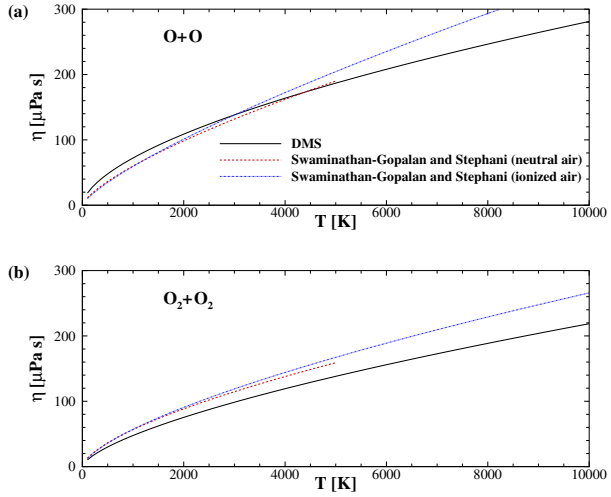

Fig. 7 Comparisons between DMS and VHS[26] oxygen shear viscosity curve fits.

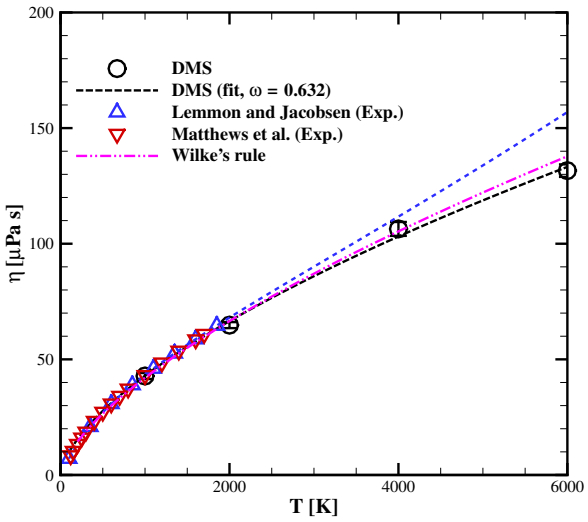

Fig. 8 DMS and experimental shear viscosity data[4,46] for non-reacting air up to 6000 K. The dashed blue line denotes the high-temperature extrapolation of the zero-density limit experimental correlation of Lemmon and Jacobsen[4].

3.3 Shear viscosity of non-reactive air

DMS predictions for viscosity of non-reacting air are shown in Fig. 8. Similarly to molecular oxygen, multiple PESs (Sec. 2.2) were required to describe the various interactions in the flow, namely N_2+N_2 (1 PES), O_2+O_2 (3 PESs), and N_2+O_2 (1 PES). As illustrated, the agreement with the experimental correlation of Lemmon and Jacobsen[4] is very good up to about 4000 K. We also report the experimental data of Matthews *et al.*[46] that extend to relatively high temperatures (up to 1700 K). A fit of the DMS data, once again using Eq. 2, yielded a shear viscosity index of 0.632 and a reference shear viscosity η_{REF} of 18.9 μPa s. Finally, the application of Wilke's rule[33], using mole fractions of 25% and 75% for O_2 and N_2, respectively, appears to predict the viscosity of air quite well up to about 4000 K, although a slightly larger discrepancy is predicted at 6000 K.

4 Conclusions

In this work, we have used the DMS method to obtain shear viscosity data for air and its components at temperatures up to 10000 K. The only input in the calculations are the *ab initio* PESs that describe the various atomic-level interactions[9–11,14]. Isothermal, plane Poiseuille flows at subsonic conditions were simulated using DMS and shear viscosity was estimated using the analytic solution of the Navier-Stokes equations.

In all cases, the DMS shear viscosity predictions for molecular systems are in excellent agreement with the experimental data[4], up to about 2000 K. Even though these potential energy surfaces were produced with a particular focus on high-energy collisions characteristic of high-temperature gaseous environments, the accuracy of the low-temperature shear viscosity data lends further credibility to their overall accuracy to describe interactions between ground-state air molecules over a wide range of collision energies.

The results for pure molecular nitrogen and pure molecular oxygen agree very well with previous QCT calculations based on the same PESs. The QCT data for molecular oxygen were obtained on the triplet O_2+O_2 surface only[21]. The agreement with DMS, that was based on all three O_2+O_2 surfaces, indicates that the three ground-state PESs predict very similar viscosity cross-sections. This precise agreement with QCT was not found for the atomic systems though, and the cause of this discrepancy is currently unknown.

The role of electronic excitation is known to be important at high temperatures. Via comparisons with theoretical data that do include electronically excited states[38], we determined that the DMS ground-state only predictions underestimate shear viscosity by at most 15% at the highest temperature considered here, namely 10000 K. However, the many simplifying modeling assumptions required in the Chapman-Enskog theory[38] limit the general validity of this conclusion, although the qualitative trends appear to be correct.

A comparison with best fits of Swaminathan-Gopalan and Stephani[26] reveals that the *ab initio* predictions for shear viscosity are generally lower than the values used in popular thermochemical nonequilibrium CFD codes[44,45]. This is of particular relevance at high temperatures, where the difference in shear viscosity ex-

ceeds 20%.

Finally, similar to our previous work[24], we verified the accuracy of Wilke's mixing rule by comparing shear viscosity values computed by the mixing rule using the pure component data only and the corresponding results from DMS. Wilke's mixing rule yields consistent predictions for the shear viscosity of non-reacting air up to about 4000 K, although a slightly larger discrepancy is observed at 6000 K.

Author Contributions

The authors confirm contribution to the paper as follows: P. Valentini (conceptualization, data curation, formal analysis, investigation, methodology, validation, writing – original draft preparation, and writing – review and editing), A. M. Verhoff (project administration, conceptualization, data curation, formal analysis, investigation, methodology, validation, and writing – review and editing), M. S. Grover (writing – review and editing), and N. J. Bisek (funding acquisition, project administration, and writing – review and editing).

Data availability

The data that support the findings of this study are available from the authors upon reasonable request.

Conflicts of interest

There are no conflicts to declare.

Acknowledgements

We acknowledge the support by U.S. Air Force Office of Scientific Research under contract LRIR 21RQCOR045 monitored by Dr. Sarah Popkin. We would like to thank the Texas Advanced Computing Center (TACC) and the DoD HPC Modernization Program for providing the computational resources for this work.

Notes and references

1 J. J. D. Anderson, *Hypersonic and High-Temperature Gas Dynamics, AIAA Education Series, 2nd Ed.*, American Institute of Aeronautics and Astronautics, Inc., Reston, VA, 2006.

2 E. Vogel, *Berichte der Bunsengesellschaft für physikalische Chemie*, 1984, **88**, 997–1002.

3 W. A. Cole and W. A. Wakeham, *J. Phys. Chem. Ref. Data*, 1985, **14**, year.

4 E. W. Lemmon and R. T. Jacobsen, *Int. J. Thermophys.*, 2004, **25**, 21–69.

5 S. Saxena and S. Chen, *Mol. Phys.*, 1975, **29**, 1507–1519.

6 F. M. Faubert and G. S. Springer, *J. Chem. Phys.*, 1972, **57**, 2333–2340.

7 P. W. Schreiber, A. M. Hunter and K. R. Benedetto, *Phys. Fluids*, 1971, **14**, 2696–2702.

8 Y. Paukku, K. R. Yang, Z. Varga and D. G. Truhlar, *J. Chem. Phys.*, 2013, **139**, 044309.

9 J. D. Bender, P. Valentini, I. Nompelis, Y.Paukku, Z. Varga, D. G. Truhlar, T. E. Schwartzentruber and G. V. Candler, *J. Chem. Phys.*, 2015, **143**, 054304.

10 Y. Paukku, K. R. Yang, Z. Varga, G. Song, J. D. Bender and D. G. Truhlar, *J. Chem. Phys.*, 2017, **147**, 034301.

11 Y. Paukku, Z. Varga and D. G. Truhlar, *J. Chem. Phys.*, 2018, **148**, 124314.

12 Z. Varga, Y. Paukku and D. G. Truhlar, *J. Chem. Phys.*, 2017, **147**, 154312.

13 J. Li, Z. Varga, D. G. Truhlar and H. Guo, *J. Chem. Theory and Comput.*, 2020, **16**, 4822–4832.

14 Z. Varga, R. Meana-Pañeda, G. Song, Y. Paukku and D. G. Truhlar, *J. Chem. Phys.*, 2016, **144**, 024310.

15 Z. Varga and D. G. Truhlar, *Phys. Chem. Chem. Phys.*, 2021, **23**, 26273–26284.

16 W. Lin, Z. Varga, G. Song, Y. Paukku and D. G. Truhlar, *J. Chem. Phys.*, 2016, **144**, 024309.

17 P. Valentini, T. E. Schwartzentruber, J. D. Bender, I. Nompelis and G. V. Candler, *Phys. Fluids*, 2015, **27**, 086102.

18 P. Valentini, T. E. Schwartzentruber, J. D. Bender and G. V. Candler, *Phys. Rev. Fluids*, 2016, **1**, 043402.

19 M. S. Grover, T. E. Schwartzentruber, Z. Varga and D. G. Truhlar, *J. Thermophys. Heat Tr.*, 2019, 1–11.

20 M. S. Grover, E. Torres and T. E. Schwartzentruber, *Phys. Fluids*, 2019, **31**, 076107.

21 T. Mankodi, U. V. Bhandarka and R. S. Myong, *Phys. Fluids*, 2020, **32**, 036102.

22 D. Bruno, A. Frezzotti and G. P. Ghiroldi, *Phys. Fluids*, 2015, **27**, 057101.

23 S. Subramaniam, R. L. Jaffe and K. A. Stephani, *Phys. Rev. Fluids*, 2020, **5**, 113402.

24 P. Valentini, M. S. Grover, N. J. Bisek and A. M. Verhoff, AIAA SCITECH Forum, 2022, p. 0875.

25 P. Valentini, M. S. Grover, N. J. Bisek and A. M. Verhoff, *Phys. Rev. Fluids*, 2022, **7**, L071401.

26 K. Swaminathan-Gopalan and K. A. Stephani, *Phys. Fluids*, 2016, **28**, 027101.

27 G. E. Palmer and M. Wright, *J. Thermophysics Heat Tr.*, 2018, **17**, 232–239.

28 M. Capitelli and R. S. Devoto, *Phys. Fluids*, 1973, **16**, 1835–1841.

29 A. B. Murphy and C. J. Arundell, *Plasma Chem Plasma P.*, 1994, **14**, 451–490.

30 P. Valentini, M. S. Grover, N. Bisek and A. Verhoff, *Phys. Fluids*, 2021, **33**, 096108.

31 G. A. Bird, *Molecular Gas Dynamics and Simulation of Gas Flows*, Cambridge University Press, Cambridge, England, 1994.

32 D. G. Truhlar and J. T. Muckerman, *Atom-Molecule Collision Theory: A Guide for the Experimentalist*, Plenum Press, New York, NY, 1979, p. 505.

33 J. O. H. C. F. Curtiss and R. B. Bird, *Molecular Theory of Gases and Liquids, Structure of Matter Series*, John Wiley and Sons Inc., Hoboken, NJ, 1964.

34 T. E. Schwartzentruber, M. S. Grover and P. Valentini, *J. Thermophysics Heat Tr.*, 2018, **32**, 892–903.

35 E. Torres and T. E. Schwartzentruber, *Theor. Comp. Fluid Dyn.*, 2022, 1–40.

36 E. Torres and T. E. Schwartzentruber, *J. Thermophysics Heat Tr.*, 2020, **34**, 801–815.

37 D. Frenkel and B. Smit, *Understanding Molecular Simulation: From Algorithms to Applications*, Academic Press, San Diego, CA, 2002.

38 V. A. Istomin and E. V. Kustova, *Phys. Plasmas*, 2017, **24**, 022109.

39 Z. Varga, Y. Shu, J. Ning and D. G. Truhlar, *Electron. Struct.*, 2022, **4**, 047002.

40 R. A. Granger, *Fluid Mechanics*, Dover Publications, 1995, p. 547.

41 R. L. Jaffe, M. Grover, S. Venturi, D. W. Schwenke, P. Valentini, T. E. Schwartzentruber and M. Panesi, *J. Thermophysics Heat Tr.*, 2018, **32**, 869–881.

42 M. S. Grover and P. Valentini, *Phys. Fluids*, 2021, **33**, 051704.

43 S. Venturi, R. L. Jaffe and M. Panesi, *J. Phys. Chem. A*, 2020, **124**, 5129–5146.

44 K. B. Thompson, B. R. Hollis, C. O. Johnston, B. Kleb, V. R. Lessard and A. Mazaheri, *LAURA Users Manual: 5.6*, NASA, Langley Research Center, Hampton, VA 23681-2199, 2020.

45 M. J. Wright, T. White and N. Mangini, *Data Parallel Line Relaxation (DPLR) Code User Manual Acadia - Version 4.01.1*, NASA, Ames Research Center, Moffett Field, CA, 2009.

46 G. P. Matthews, C. M. S. R. Thomas, A. N. Dufty and E. B. Smith, *J. Chem. Soc., Faraday Trans. 1*, 1976, **72**, 238–244.